INTERNATIONAL ATOMIC ENERGY AGENCY
UNITED NATIONS EDUCATIONAL, SCIENTIFIC AND CULTURAL ORGANIZATION

INTERNATIONAL CENTRE FOR THEORETICAL PHYSICS
34100 TRIESTE (ITALY) - P.O.B. 586 - MIRAMARE - STRADA COSTIERA 11 - TELEPHONE: 2240-1
CABLE: CENTRATOM - TELEX 460392-1

SMR/406-11

THIRD AUTUMN WORKSHOP ON ATMOSPHERIC
RADIATION AND CLOUD PHYSICS
27 November - 15 December 1989

"Radiative Transfer of Cirrus Clouds"

Steven A. ACKERMAN
University of Wisconsin Madison
Space Science and Engineering Center
Madison, Wisconsin
USA

Radiative Properties of Cirrus Clouds

Steven A. Ackerman

Cooperative Institute for Meteorological Satellite Studies

1225 West Dayton St.

University of Wisconsin-Madison, Madison, WI. 53706

(November 1989)

1. INTRODUCTION

The importance of clouds in climate research is well recognized and much attention has been given to the radiative properties of clouds and their parameterization. Cirrus clouds significantly alter the radiative heating and cooling of the atmosphere and at the earth's surface, thereby affecting atmospheric circulations. Cirrus clouds also undergo physical changes (e.g. particle size distribution, ice water content and cloud top and base altitude) as they form, grow and dissipate. These physical changes are capable of affecting the radiative characteristics of the cloud. Radiative processes have a strong influence on the convective structure and ice water budget of cirrus clouds (Starr, 1987). Radiative processes also effect the particle growth rate (Stephens, 1983). Recent advances in instrumentation and theory have led to a significant increase in our understanding of the coupling of the microphysical and radiative properties of cirrus clouds. We will be focusing on the interdependance of the these properties.

2. Single Scattering Properties

Before discussing the transport of energy through clouds, we need first to consider the scattering properties of a single particle. Rather than present a complete theoretical treatment of scattering, we will consider some important aspects of the results of the theory and how they

apply to cirrus clouds. The parameters needed to compute the transfer of radiative energy within a layer are:

- extinction coefficient, σ_{ext} (which integrated over path length gives the optical thickness, τ). This parameter characterizes the attenuation of radiation through a cloud volume.;
- single scattering albedo, $\omega_o = \sigma_{ext}/\sigma_{sca}$. ω_o ranges between 1, for a non-absorbing medium and 0 for a medium that absorbs and does not scatter energy.
- phase function, $P(\cos\vartheta)$ which describes the direction of the scattered energy. When one is interested in fluxes it is sufficient to know the asymmetry parameter, $g = \int_{-1}^{1} P(\cos\vartheta)\mathrm{d}\cos\vartheta$ which represents the 'backward to forward' scattering ratio. It is 0 for isotropic scatter, +1 and -1 for complete scatter in the forward and backward direction respectively.

Given these single scattering properties of a layer, in addition to the radiative characteristics of the molecular atmosphere, the layer reflectance, transmittance and absorptance can be determined.

2a. Microphysics of Cirrus Clouds

There are three important physical properties of a particle that are needed to determine its single scattering properties. The shape of the particle or habit. The size parameter, which is a measure of the size of the particle in comparison to the wavelength of the incident radiation

$$\chi = \frac{2\pi r}{\lambda} \tag{1}$$

The size distribution of particles, n(r), throughout the cloud is also needed. In addition to defining the radiative properties, the n(r) also determines the ice water content of a layer (IWC=$4/3\pi\rho_{ice}\int n(r)r^3\mathrm{d}r$). For purposes of radiative transfer, it is useful to characterize the size distribution in terms of the effective radius

$$r_{eff} = \frac{\int_0^\infty \mathrm{n(r)}r^3 dr}{\int_0^\infty \mathrm{n(r)}r^2 dr} \tag{2}$$

As noted by Hansen and Travis (1974) and Ackerman and Stephens (1987), the effect of the size distribution on the single scattering properties is, for large effective size parameters ($\chi_{eff} = \frac{2\pi r_{eff}}{\lambda}$, where λ is the wavelength), primarily determined by r_{eff}.

The index of refraction of the particle is also needed

$$m = n_r - in_i \tag{3}$$

Actually we need to know the index of refraction of the medium also, but for air it is 1 so we don't worry about it, but be careful if you are doing radiative transfer in the ocean. The imaginary part is an indication of the strength of the absorption by the particle; with $n_i = 0$ there is no absorption.

2a. Microphysical properties

This section briefly discusses the cirrus cloud microphysics often assumed in radiation studies.

Measurements of the index of refraction of a material are very difficult to make (Bohren and Huffman 1983). This study uses the index of refraction of soil derived aerosols presented by Warren (1984). Figures S1 and S2 depict the real and imaginary parts of the index of refraction of ice and liquid water. Note that large difference can occur between ice and liquid water for a given wavelength; these spectral regimes have been employed to remotely sense the water phase of the cloud. For example, Pilewskie and Twomey (1987) used reflectance measurements near 1.6 and 2.2 μm for discrimination of the cloud water phase based on differences in n_i. Measurements at 1.55 and 1.25 μm of cloud reflectance can be used to distinguish ice and water clouds, although thin ice clouds overlying water clouds are not detected (Foot, 1988). Ackerman *et al.* (1989) used the 8-12 μm regions to distinguish ice clouds from liquid water clouds. There are also regions in n_r that change sharply over a small wavelength range (e.g. 2.75-3.25 μm and 10-14 μm). Changes in n_r change the relative locations of the maximum and minimum in the volume extinction coefficients and are potential spectral regions for remote sensing particle size distribution or the effective radius of the distribution.

Ice particle shapes (habits) are often derived from 2D probe data or direct collections of particles on oil-coated slides. The 2D Probes detect particles that are larger than 25-50 μm by imaging the cross-sectional area of the particle. An example of particle shapes observed under ideal conditions of a lab are given in figure S3. Microscopic analysis reveals that the cirrus cloud particles

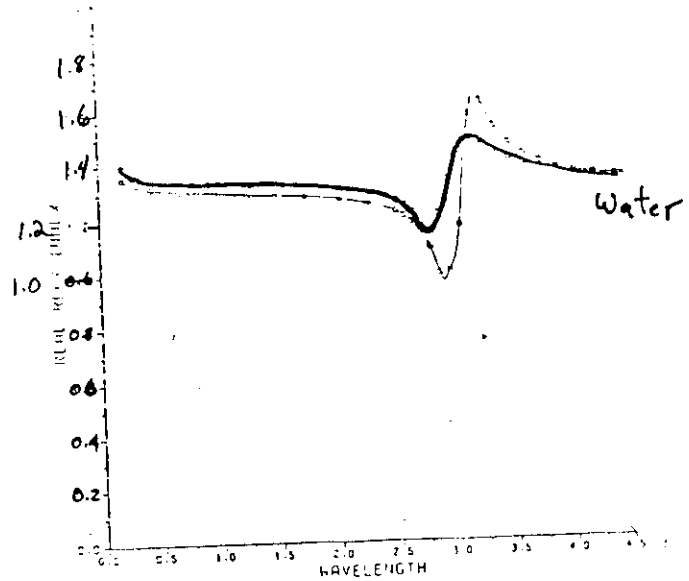

FigureS1a: Real Part of Complex Index of Refraction of Water and Ice (water uses □; ice uses o) over 0.2-4.5 μm.

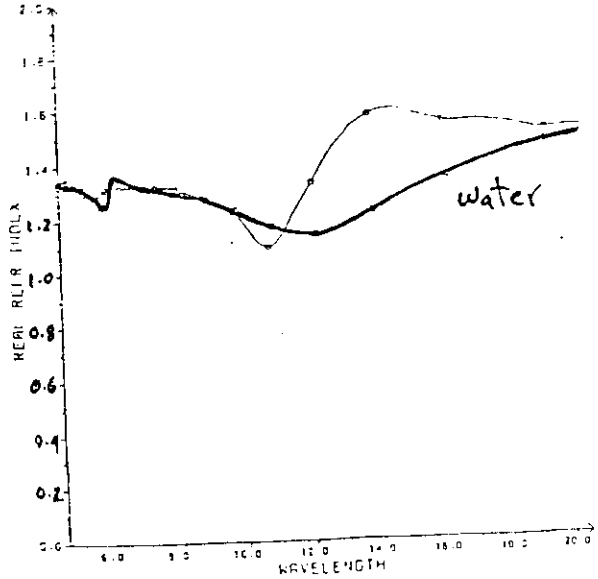

FigureS1b: Real Part of Complex Index of Refraction of Water and Ice (water uses □; ice uses o) over 4.0-20.0 μm.

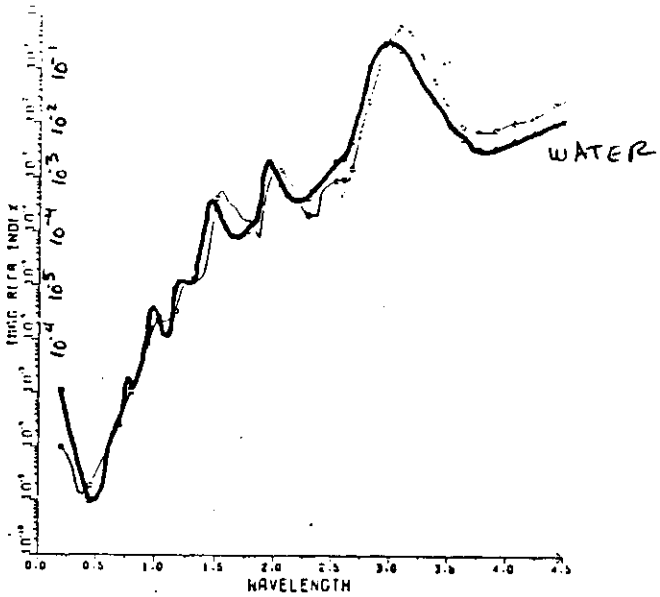

Figure 2a: Complex Part of Complex Index of Refraction of Water and Ice (water uses □; ice uses o) over 0.2-4.5 μm.

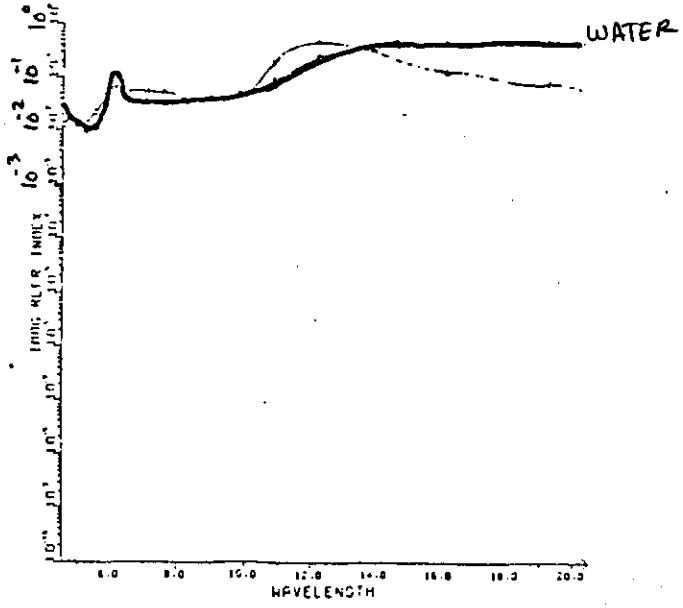

Figure 2b: Complex Part of Index of Refraction of Water and Ice (water uses □; ice uses o) over 4.0-20.0 μm.

Figure 3: A classification of ice particle types.

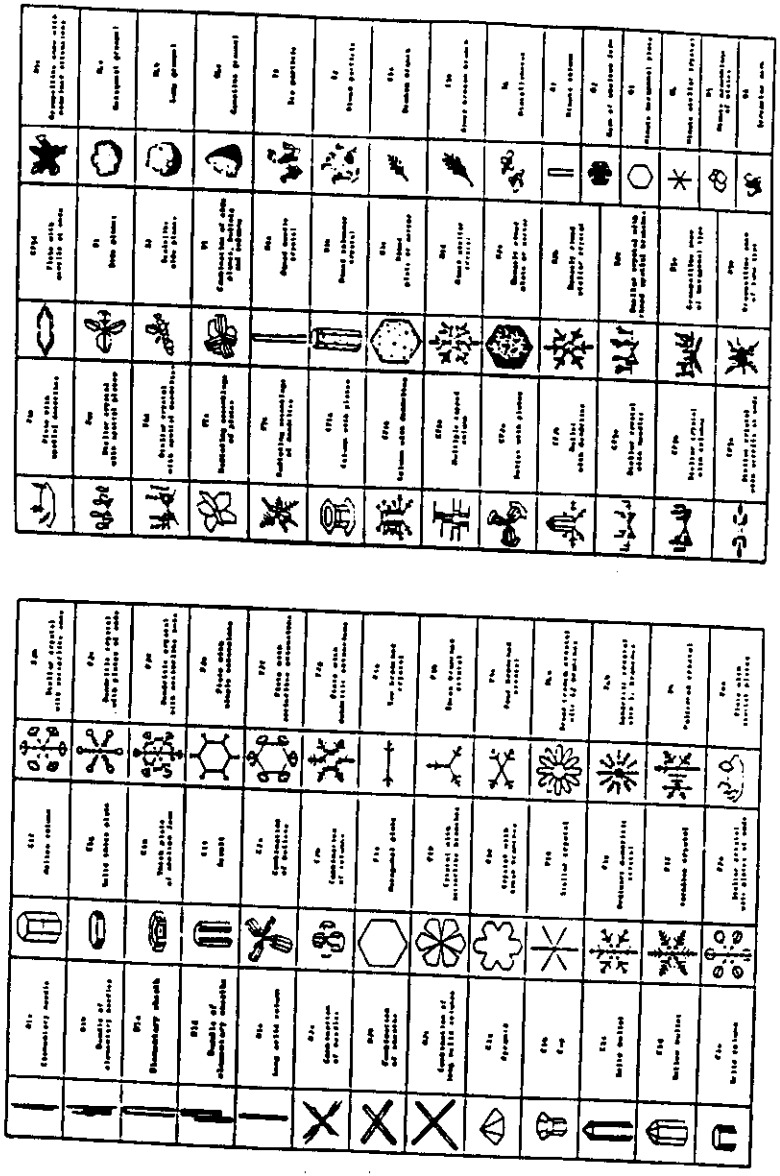

are often irregular in shape, though distinct shapes can be seen. Ice crystal size distributions in cirrus can vary by more than an order of magnitude; however, there have been several observation programs which have produce extremely useful size distributions for radiative transfer calculations. Heymsfield and Knollenberg (1972) measured the microphysics of cirrus clouds and found mean crystal lengths of 60 -1000 μm with IWC of 0.15-0.25 gm^{-3}. The dominant particle shapes where columns, bullets, rosettes and plates. Hobbs *et al.* (1975) measured columns, plates and bullets in cirrostratus, cirrocumulus and cirrus. Sizes ranged form 100-1000 μm with IWC form 0.006 to 0.3 gm ^{3}. Heymsfield (1975, 1977) found that the most common shapes in cirrus uncinus and cirrostratus where bullet rosettes, single bullets, banded columns and plates. Typical ice crystal size distribution measured by Heymsfiel (1975) is shown in figure S4. His measurements also suggested the presence of smaller crystals with sizes less than 50μm.

As noted above, the ice water contents (IWC) of cirrus clouds can also vary an order of magnitude and can display a large horizontal variation within a given cloud. Though the variability is large, several generalizations can be made which are useful for radiative transfer calculations. The IWCs often are larger near the cloud base than near the cloud top. Observations of Heymsfield (1975, 1977) depicted a dependency of IWC and the mean crystal length on temperature. This relationship was further explored by Heymsfield and Platt (1984). Figure S5, depicts the average particle spectra as a function of temperature range. For particle dimension in the range 20 -300 μm two grouping are seen; The first is for the -20° to - 40° C range and the second which exhibits smaller concentrations, is for colder temperatures. Distributions with larger maximum dimensions display more dependency on temperature.

Hemysfield and Platt (1984) also noted a dependency of the IWC as a function of ambient temperature (Figure S6). While there is a tendency of increasing IWC with increasing temperature, variations at a given temperature can be an order of magnitude. Still this relationship is useful for theoretical studies and radiative parameterizations as we shall see later.

2.b The effect of particle shape and size

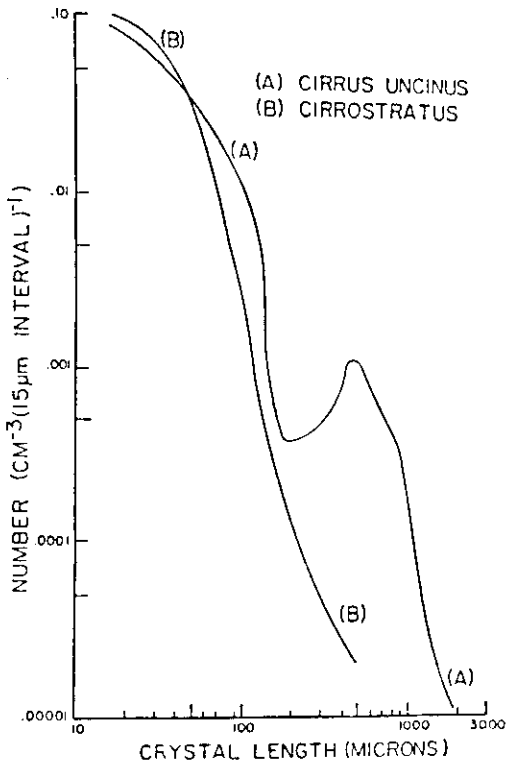

FIG. 4. Ice crystal size distributions for cirrus clouds. (After Heymsfield, 1975a.)

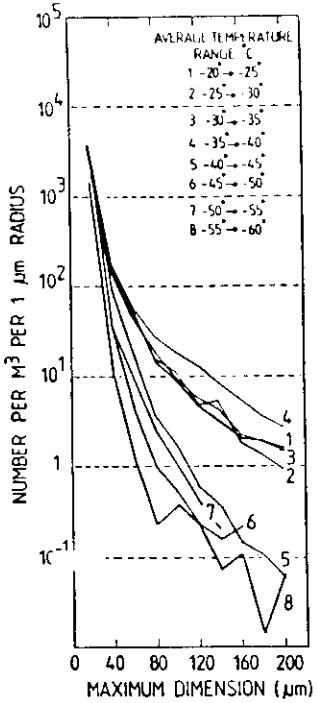

FIG. 5a. Average particle spectra in different temperature ranges for the 20–300 μm crystal maximum dimension.

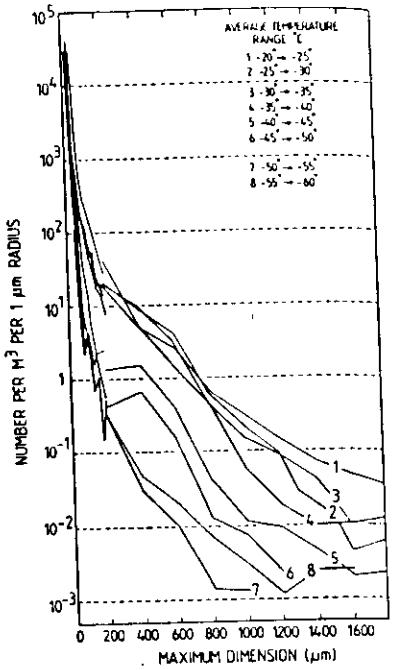

FIG. 5b. As in Fig. but for 20–1800 μm maximum dimension.

After Heymsfield and Platt (1984)

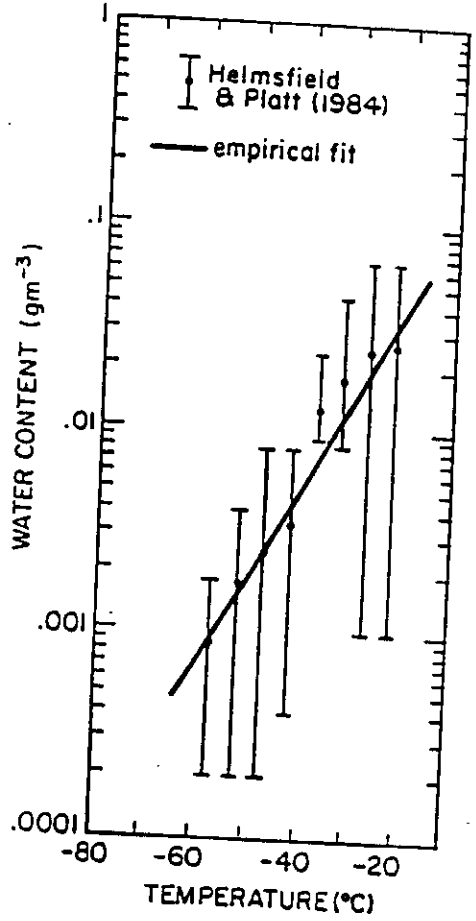

figure 5b.

The exact solution of the electromagnetic wave equation for scattering by spheres was presented by Mie (1908), while more recent solutions have been obtained for prolate and oblate spheroids (Asano and Yamamoto, 1975), and for infinitely long cylinders (Wait, 1955; Liou, 1972). These solutions are both mathematically cumbersome and computationally tedious. Lacking a general solution to the scattering by irregularly shaped particles, theoretical calculations generally assume one of three particle shapes; spheres, cylinders or hexagonal columns. The most common particle shape assumed in radiative transfer studies is the sphere. Even when it is know that the particles are non-spherical, an **equivalent size sphere** or effective radius is often sought which produces the observed radiative observations. It is also instructive to use spheres to understand the effect of particle size and n(r) on the single scattering properties of a layer. Some of the more important relationship between particle size and single scattering properties are listed below:

- A small dispersion of sizes washes out the ripple structure
- The effect of different sizes is to damp the max and min
- Absorption also damps the major maxima and minima
- For $\chi \geq 10, \omega_o$ is practically independent of the width of the size distribution, b
- Maxima and Minima in g have the same origin as in Q_{sca}
- For small particle g approaches 0
- For visible and near IR wavelengths, g is nearly independent of the variance in n(r)
- For large values of χ, $g \rightarrow 1$ as $n_r \rightarrow 1$ while as $n_r \rightarrow \infty$ $g \rightarrow 0.5$, due to diffraction.

Unlike the scattering properties of spheres, the scattering by non-spherical ice particles is largely unknown, though the properties above appear to be consistent with non-spherical particles. Since column like features are often observed, the scattering properties of circular cylinders (Kerker, 1969 and Liou 1972a and b) have often been used to study cirrus clouds (Liou 1972b, Stephens 1980). When compared to ice spheres, long ice cylinders scattered more light in the side directions at the expense of scattering in both the forward and backward directions. Thus the largest difference in the bulk radiative properties of clouds consisting of spheres and of cylinder is for reflectance, which is a function of the degree of anisotropy of the scatter. Observed relation between albedo and emittance suggests that theoretical treatment of cirrus ice particles as cylinders is better than treatment as equivalent spheres (Paltridge and Platt, 1981).

The scattering properties of hollow cylinders was studied by Stephens, (1987). The scattering properties of a distribution of hollow cylinders were not greatly different from a distributions of equivalent homogeneous cylinders. The effect of a hollow distribution on the radiative properties of a cloud was primarily due to its effect on the ice water path (IWP=$\int IWC dz$) and not on the single scattering properties of the cloud (Stephens, 1987).

Single scattering properties have also been computed for hexagonal ice columns (Jacobowitz, 1971; Wendling et al , 1979; Liou and Coleman, 1980, Takano and Liou, 1988). These regularly shaped particles are often assumed to represent the average thin cirrus clouds, since some cirrus produce optical phenomena such as the 22° halo, which are produced by hexagonal columns.

Solutions for other symmetrical particles have been presented in the literature (Ansan and Sato, 1980;), but these solutions have not yet been applied to cirrus clouds. Primarily because of there application to small size parameters or there computational expense. For irregular large weakly absorbing particles the scattering coefficient depends upon the cross-sectional area while the absorption coefficient should depend on the volume of the particle.

The largest effect on particle shape is on the phase function. Figure S7 depicts phase functions of four particle habits (Foot, 1988). Spherical particles show the lowest side scattering and the rainbow. The hexagonal ice columns depict the 22° halo and more side scatter than the spheres. The experimental curves (Sassen and Liou, 1979; Volkovitskiy, *et al.*, 1980) exhibit less variation and larger values at side scattering angles. These experimental observations tend to agree better with aircraft an satellite observations (Foot, 1988; Wielicki *et al.*, 1989) than the theoretical values.

In summary, the particle habit appears to have its greatest impact on the phase function. The bulk radiative properties of cirrus clouds are less sensitive to assumptions about the scattering phase function than vertical radiance measurements.

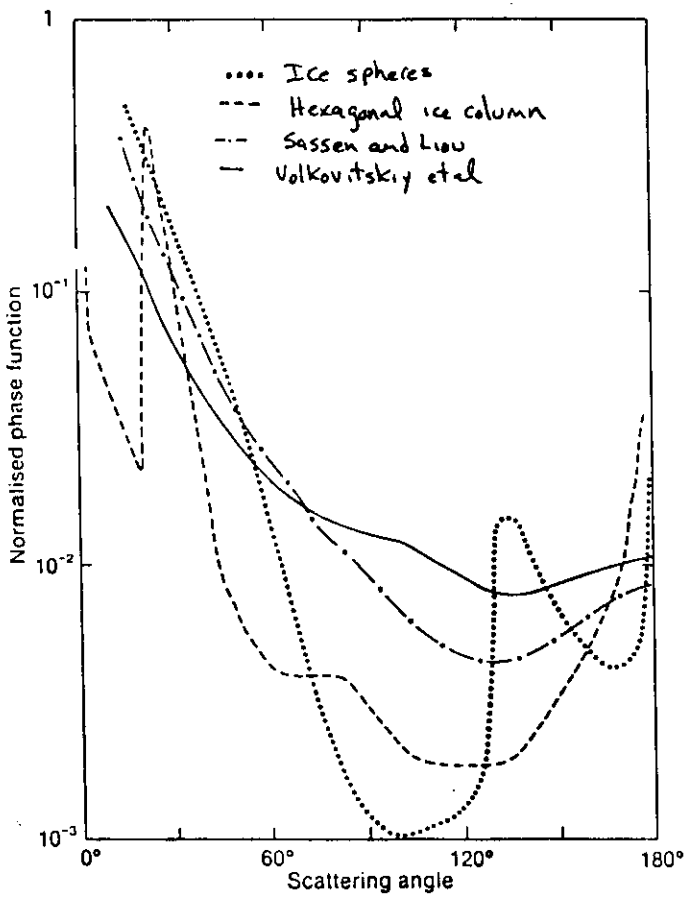

figure 57

3. Radiative Properties

Because of the frequent occurrence and persistence in time, their large areal extent and location high in the troposphere cirrus clouds are important radiative features of the earth/atmosphere system. In this section we discuss the observations and theoretical calculations of the radiative properties of cirrus.

3a. LW Radiative Properties

Airborne observations of the effects of cirrus clouds on the thermal radiation budget have been made since the late 1950's (Brewer and Houghton, 1956; Gates and Shaw, 1960; Fritz and Rao, 1967; Kuhn, 1970; Kuhn and Weikman, 1969). These early studies demonstrated that cirrus clouds can not be considered black in the infrared. A common method of describing the infrared properties for clouds from flux measurements is the effective emissivity, defined as

$$\varepsilon^* \downarrow = \frac{F\downarrow(\tau_b) - F\downarrow(\tau_t)}{B(T) - F\downarrow(\tau_t)} \tag{4}$$

and

$$\varepsilon^* \uparrow = \frac{F\uparrow(\tau_t) - F\uparrow(\tau_b)}{B(T) - F\uparrow(\tau_b)} \tag{5}$$

The need for separate emissivities for the upward and downward directions is related to differences in the spectral distribution of the energy at the layer boundaries, and has be discussed by Rodgers (1967), Cox (1971, 1976) and Stephens (1979). Expressions of the form of equations (4) and (5) have been applied to aircraft observations to derive effective emissivities. Observations (Cox, 1971) and calculations (Stephens, 1979) indicate that for water clouds $\varepsilon^*\downarrow > \varepsilon^*\uparrow$. Equations (4) and (5) do not include any dependency on the particle size distribution.

The main difference between the two effective emissivities occurs in the 8-12 μm window where the upward flux at the layer base is related to the surface temperature via the spectrally integrated Planck function and surface emissivity. The downward irradiance originates from a O_3 contribution near 9.6 μm and is much smaller. The effect of a cloud layer on the radiative fluxes is a function

of its emissivity and the layer temperature (assumed isotropic). In the case of the upward flux the warm surface temperature is replaced by a cold cloud, only slightly modifying the energy. However, the downward incident flux at the top of the cirrus cloud is small and the presence of the cloud can cause a large change in the downward flux through the Planck function. A cloud is therefore more efficient in modifying the downward irradiance and has a higher gray body emissivity for this direction than for the upward direction. The cloud broadband flux effective emissivity as a function of pressure for midlatitude and tropical radiometersonde observations has been presented by Cox (1976). These observations showed a wide variability in ε^* and demonstrated that cirrus cloud effects on climate was dependent on the latitude.

Aircraft observations in the 1970's were better able to define the relationship between a clouds infrared properties and its microphysical ones. The effective emissivity was often parameterized in terms of the IWC as

$$\varepsilon^* = 1 - \exp(-K(\int IWC\,\mathrm{d}z)) \tag{6}$$

where K is the broadband mass absorption coefficients. Observations of K for tropical cirrus ranged from 0.076 to 0.096 $m^2 g^{-1}$ in the measurements of Griffith *et al.* (1980). Paltridge and Platt (1981) measured and average value for cirrus over New Mexico of 0.056 $m^2 g^{-1}$. Observations of Smith *et al.* (1988) ranged from 0.046-0.18 $m^2 g^{-1}$ for observations over Wisconsin. This parameterization assumes that the emissitivity is also independent of particle size. Recent observations by Smith *et al.* (1988) indicate that K varied in an inverse way with the measured maximum crystal dimension. While Foot (1988) found the cirrus emission to be more closely related to the total cross-sectional area of the particles in a column than to the IWP; however, horizontal variation in cloud structure made it difficult to relate the optical depth to the cross-sectional area of the particles. Discrepancies exist between these reported value of effective emissivities and theoretical values. Part of this difference can be attributed reflectance by the cloud. Figure R1 depict the downward and upward broad-band emittance as a function of IWP from theoretical calculations of Stephens (1980). The dashed curves are the ε^* which combines emission and reflection while

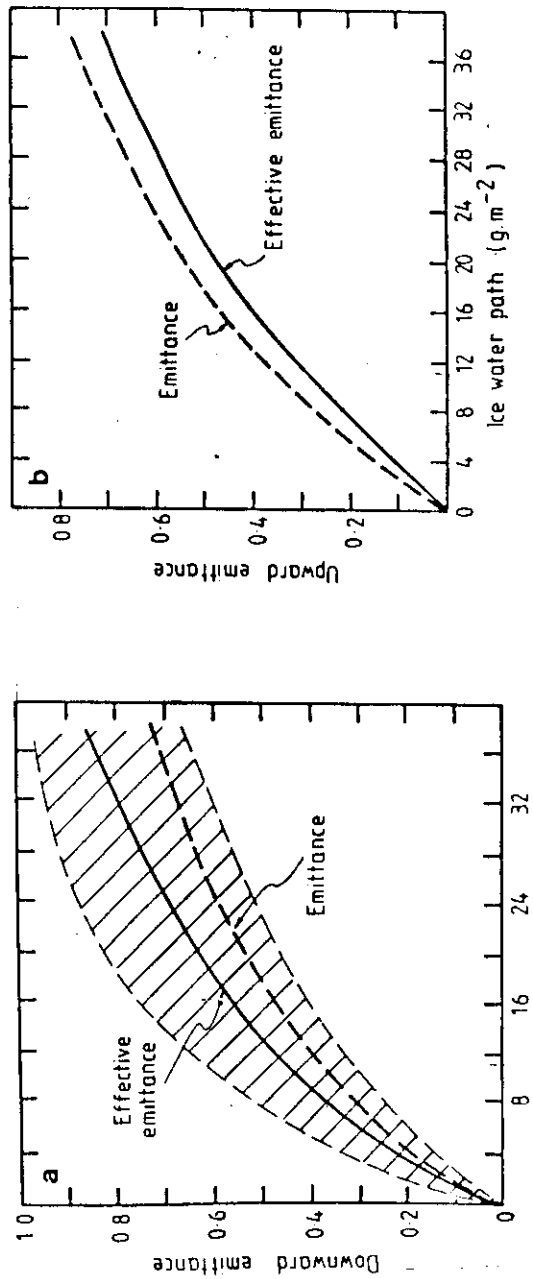

figure R1 after Stephens (1980)

the solid lines are cirrus cloud emittance. The differences, which are significant, demonstrate the effect of IR reflectance on the assumed emittance. The shaded region represent the relationship of Giffith *et al* (1980). The existence of IR reflectance from cirrus clouds may account for discrepancies in the broad band effective emittances derived from observed flux profiles and theoretical calculations.

Effective beam spectral emittances, for the vertical direction, have also been derived from aircraft observations and parameterized as a function of IWP. Often a wavelength of approximately 11 μm is chosen for such studies as it is a window region and assumed representative of satellite instruments. Figure R2 is the relationship derived by Paltridge and Platt (1981). The effect of scattering also plays an important for these spectral emittances. IR reflectance at 11 μm at cloud base is 4% for spheres and 6% for random oriented cylinders (Stephens, 1980). Conversion between the beam emissivity and a flux emissivity is often achieved by assuming a diffusivity factor of 1.66. Aircraft observations have been used to derive empirical relations between the broadband infrared flux emittance and the 11 μm beam emittance (Figure R3).

Effective emittance is not as useful for high clouds as it is for low-level water clouds because of the temperature difference between the cloud and the surface. Due to the large temperature difference, a small reflectance can result in a large contribution to the downward irradiance at the cloud base. To demonstrate the effect of reflectance and particle size on cirrus cloud emittance it is useful to consider the two stream solution of the radiative transfer equation appropriate for thermal source. While various solutions exist, here we consider the form (Geleyn and Hollingsworth,1979; Ackerman and Cox, 1987)

$$\begin{bmatrix} F\downarrow(\tau_t) \\ F\uparrow(\tau_t) \end{bmatrix} = \begin{bmatrix} t & r \\ r & t \end{bmatrix} \begin{bmatrix} F\downarrow(\tau_t) \\ F\uparrow(\tau_b) \end{bmatrix} + \begin{bmatrix} s-t & 1-s-r \\ 1-s-r & s-t \end{bmatrix} \begin{bmatrix} B(\tau_t) \\ B(\tau_b) \end{bmatrix} \tag{7}$$

where

$$r = \frac{\varrho(1-e^{-\tau_{*II}})}{1-\varrho^2 e^{-\tau_{*II}}} \tag{8}$$

$$t = \frac{e^{-\tau_{*II}}(1-\varrho^2)}{1-\varrho^2 e^{-\tau_{*II}}} \tag{9}$$

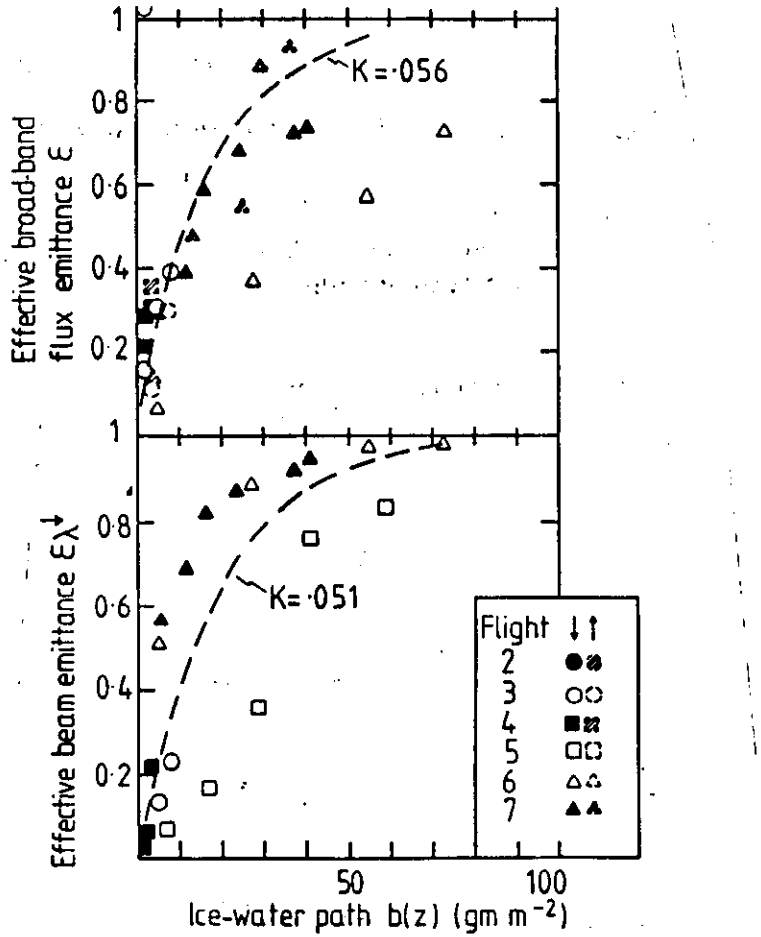

figure R2 (Paltridge and Platt, 1981)

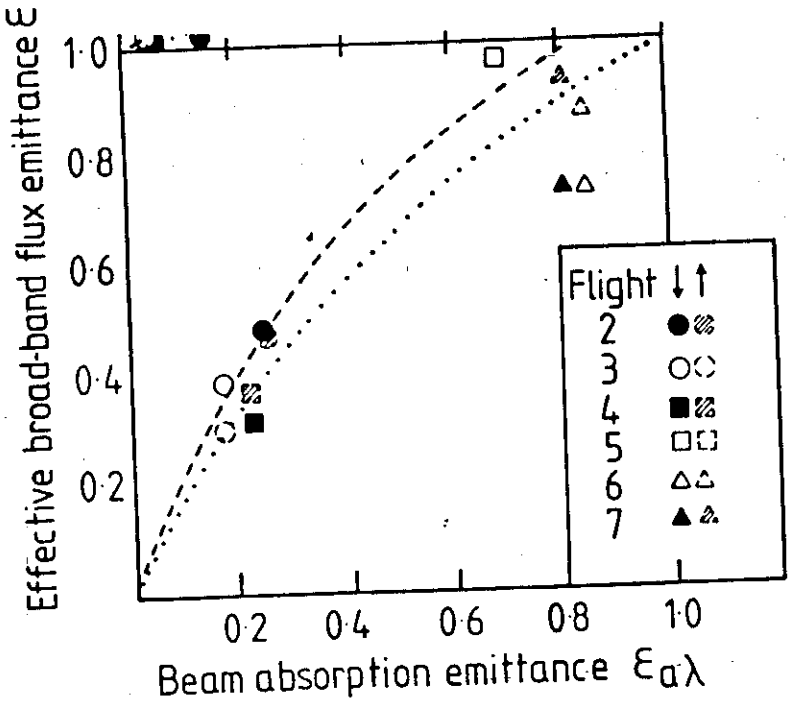

figure R3

$$s = \frac{(1 - t + r)}{\bar{\mu}(1 - \omega_0 + 2\omega_0\bar{\beta})\tau} \tag{10}$$

$$K = \sqrt{1 - 2\omega_0 + \omega_0^2 + 2\omega_0\bar{\beta} - 2\omega_0^2\bar{\beta}} \tag{11}$$

$$\tau_{eff} = \bar{\mu}K\tau = \pi\bar{\mu}\int\int KQ_{ext}\mathrm{n(r)r^2\,dr\,dz} \tag{12}$$

$$\varrho = \frac{\omega_0\bar{\beta}}{1 - \omega_0 + \omega_0\bar{\beta} + K} \tag{13}$$

where B is the Plank function $\bar{\beta}$ is the backscatter coefficient (Wiscombe and Grams, 1976) and $\bar{\mu}$ is the diffusivity factor ($\bar{\mu} \approx 1.66$). For an isothermal cloud, $B(\tau)$, equations (7)-(13) indicate the necessity to parameterize two variables, ϱ and KQ_{ext}. Physically, ϱ is the reflectance for an infinitely thick cloud. The value of ϱ for ice spheres as a function of wavelength is shown in figure R4 for three particle sizes: 5 μm (square), 10μm (circle), and 30μm (triangle). For wavelengths between 10 and 13 μm, ϱ is a weak function of particle size and $\varrho < 0.08$. ϱ can become large for small particles for regions outside this window.

A effective emittance follows directly from the LW two-stream model by assuming that $r \approx 0$, which requires $\varrho \approx 0$ such that

$$\epsilon^* = 1 - t = 1 - \exp(\bar{\mu}\pi\int\int KQ_{ext}\mathrm{n(r)r^2dr\,dz}) \tag{14}$$

which is the common form used in both theoretical studies and aircraft observations. It is therefore important to parameterize the quantity KQ_{ext}. In the absence of scattering,

$$KQ_{ext} = Q_{abs} \tag{15}$$

Figure R5 depicts the ratio of KQ_{ext} to Q_{abs} as a function of wavelength for three particle sizes, 5 μm (square); 10μm (circle); and 30μm (triangle). For wavelengths greater than 10μm, $KQ_{ext} \approx Q_{abs}$. This ratio displays a similar dependency on wavelength and droplet size as that depicted by ϱ. In studying the longwave properties of clouds, it is therefore useful to parameterize Q_{abs}. It is often assumed (Platt, 1976; Chýlek 1978; Pinnick *et al.* 1979) that $KQ_{ext} \approx Q_{abs}$ and

$$Q_{abs} \approx \mathrm{cr} \quad \text{for } \mathrm{r} < \mathrm{r}_m \tag{16}$$

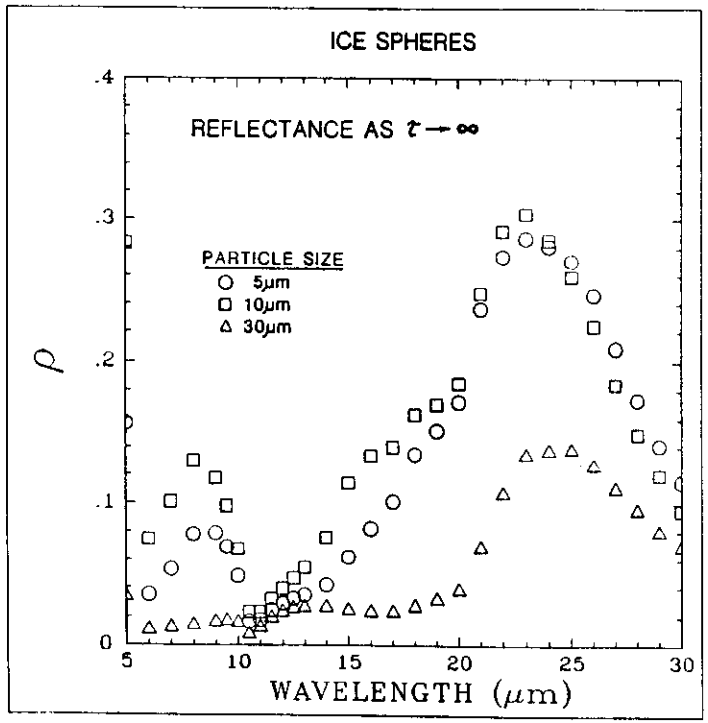

figure R4

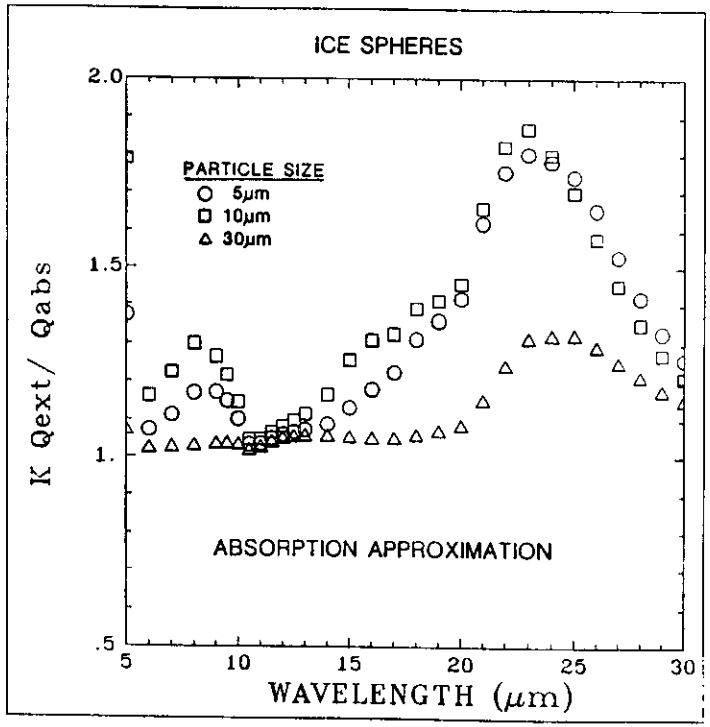

figure R5

which leads to the empirical parameterization derived by aircraft observations in the 1970's (e.g. Paltridge, 1974; Platt, 1976; Stephens *et al.*, 1978; Griffith *et al.*, 1980; Paltridge and Platt, 1981; Schmetz *et al.*, 1981;):

$$\epsilon^* = 1 - \exp(-K\ LWP) \tag{17}$$

where LWP is the liquid water path of the cloud ($\frac{4}{3}\rho_{wat}\pi \int\int n(r)r^3 dr\, dz$). There is no dependency on the particle size other than its relationship to the LWP. As discussed by Chýlek and Ramaswamy (1982) and Stephens (1984), equation (17) is strictly valid for clouds of droplets smaller than r_m, the value of which changes with wavelength. Such an approximation will break down for clouds whose size distribution contains a number of large droplets and therefore is probably not valid for cirrus clouds (Stephens, 1984) which consist of large ice crystals.

Recent aircraft observations of the radiative and microphysical properties of water clouds have demonstrated the dependency of emittance, and K, on the cloud particle size distribution. For example, Bonnel *et al.* (1980) discuss the sensitivity of the measured emittance of African and mid-latitude stratocumulus clouds to the particle size distribution. Based on observations of summertime ar ratus clouds, Curry and Herman (1985) present a parameterization of the cloud emittance in terms of the liquid water content and the droplet equivalent radius. Smith *et al* (1988) also noted a dependency of K on cirrus particle size. While the dependency between cloud emittance and particle size has been observed in measurements, as well as radiative transfer calculations, a simple parameterization scheme which describes this size dependency has yet to be presented. A common method of incorporating the size dependency is to present parameterizations as a function of cloud type. To include the effects of particle size on cloud emittance, we consider the modified anomalous diffraction theory and make use of the first order approximation $KQ_{ext} \approx Q_{abs}$.

In studying the solar radiative properties of a cirrus clouds, an appropriate approximation to Mie theory is the anomalous diffraction theory (ADT) of van de Hulst (1957). This theory is based on the assumption that the size parameter $\chi = 2\pi r/\lambda \gg 1$ where r is the particle radius and λ is

the wavelength of the incident radiation. This assumption allows ray tracing through the particle. The second requirement is that the refractive index, m, must be very close to 1 (i.e. $m - 1 \ll 1$), implying that the ray experiences only a slight deviation as it crosses the two boundaries of the particle and that the energy reflected at these boundaries is negligible. Under these assumptions, van de Hulst derived analytical expressions for the efficiency factors of extinction and absorption

$$Q_{ext} = 2 - 4e^{(-\rho\tan\beta)}\frac{\cos\beta}{\rho}\left[\sin(\rho-\beta) + \frac{\cos\beta}{\rho}\cos(\rho-2\beta)\right] + 4\left(\frac{\cos\beta}{\rho}\right)^2\cos 2\beta \tag{18}$$

$$Q_{abs} = 1 + \frac{e^{-4\chi\kappa}}{2\chi\kappa} + \frac{e^{-4\chi\kappa}-1}{8\chi^2\kappa^2} \tag{19}$$

where

$$\rho = \frac{4\pi r(m-1)}{\lambda} \tag{20}$$

$$\tan\beta = \frac{\kappa}{n-1} \tag{21}$$

Physically, the parameter ρ is the phase lag of the ray that passes through the center of the sphere. While ADT is based on the assumptions $m - 1 \ll 1$ and $\chi \gg 1$, it has often been demonstrated that the theory can successfully be applied to cases outside these limits. This simple theory can be improved upon by including edge effects and refraction of the transmitted ray (Ackerman and Stephens, 1987). For the case of the modified ADT which includes refraction (MADT) the efficiency factors for extinction and absorption are

$$Q_{ext} = 2 - \frac{4m^2}{\rho}e^{-\rho\tan\beta}\cos\rho\left[\sin(\rho-\beta) - \frac{\cos\beta}{\rho}\cos(\rho-2\beta)\right] \tag{22}$$

$$+\frac{4m^2}{\rho}e^{-\rho\sqrt{1-m^{-2}}\tan\beta}\cos\beta\left[\sqrt{1-m^{-2}}\sin(\rho\sqrt{1-m^{-2}}-\beta) + \frac{\cos\beta}{\rho}\cos(\rho\sqrt{1-m^{-2}}-2\beta)\right]$$

$$Q_{abs} = 1 + \frac{m^2}{2\chi\kappa}e^{-4\chi\kappa}\left(1+\frac{1}{4\chi\kappa}\right) - \frac{m}{2\chi\kappa}e^{-4\chi\kappa\sqrt{1-m^{-2}}}\left(\sqrt{m^2-1}+\frac{m}{4\chi\kappa}\right) \tag{23}$$

The accuracy of these approximations has been discussed by Ackerman and Stephens (1987). By expressing the particle size distribution n(r) in some analytical form (e.g. power law, log-normal or gamma distribution) one can derive analytical expressions for the volume extinction and absorption coefficients (σ_{ext} and σ_{abs} respectively).

Figure R6 depicts the relations between wavelength and Q_{abs} for two different droplet sizes. The stars represent Mie calculations while the circles denote the approximation MADT. The open symbols are for a 30μm particle while the solid symbols represent the calculations for a 1μm droplet. The approximation is excellent, even for droplets as small as 1μm. To demonstrate the dependence of effective emittance on the particle size, Q_{abs} is expressed using MADT, then

$$\epsilon = 1 - \exp\left(\bar{\mu}\pi \int\int \mathrm{n(r)} \left\{\frac{4}{3}m^2 r^3 \kappa \left[1 - (1-m^{-2})^{3/2}\right] \mathrm{dr} + \mathrm{r}^4\kappa^2 m^2 \left[1 - (1-m^{-2})^2\right]\right\} \mathrm{drdz}\right) \tag{24}$$

where $\kappa = 4\pi n_i/\lambda$ is the absorption coefficient of water. The first term of the exponential represents the dependency on the liquid water content of the cloud, while the second term displays a dependency on the fourth moment of the size distribution. The dependency between cloud emittance and particle size distribution is a function of the parameter κr. For weakly absorbing regions and small particles, $\kappa^2 r^4 << \kappa r^3$ and the effective emissivity is primarily a function of the cloud IWP. In strongly absorbing regions, large κ, the effective emissivity will be a function of droplet size. As an estimate of the particle size at which the effective emissivity becomes dependent on the droplet size we consider the radius at which

$$\frac{4}{3}m^2\kappa \left[1 - (1-m^{-2})^{3/2}\right] = \mathrm{R}\kappa^2 m^2 \left[1 - (1-m^{-2})^2\right] \tag{25}$$

Figure R7 depicts this radius, R, as a function of wavelength for water (solid lines) and ice (dashed lines) spheres. A cloud with a monomodal distribtuion of particles of size R or greater will display a sensitivity to the droplet size. For example, if we have two clouds, one with a mon-modal size distribution of 12μm particle and the other with a 8μm droplet distribution, the cloud emissivity

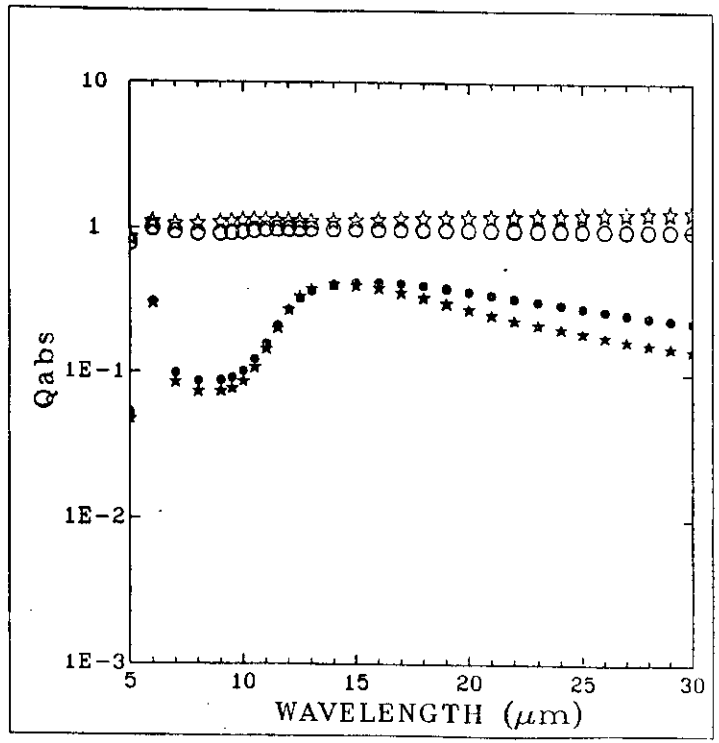

Figure R6

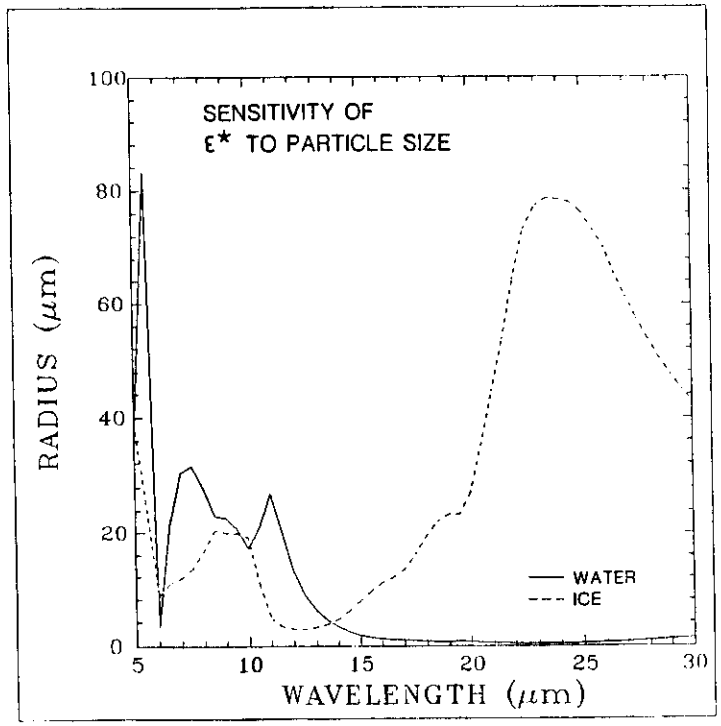

Figure 7

in the 8-11.5 μm band will be sensitive primarilly to the IWP, while the 11.5 to 14 μm band emissivity would also display a sensitivity to the size distribution. This is in agreement with the calculations of Chýlek and Ramaswamy (1982), who found that the emissivity of water clouds in the 8-11.5μm band was a function of IWP while for the 11.5-14μm the emissivity was a function of the size distribution as well. Beyond 14μm the cloud emissivity will be a funciton of the droplet size (Figure R7). In the the case of ice clouds, the 11-13 μm band will display a dependency on the size distribution for particle greater than 4 μm, and has been used by Ackerman *et al* (1989) to infer the effective radius of the size distribution from high spectral resolution IR measurements.

Alternative to equations (4) and (5), the effective emissivity for a non- isothermal cloud can be written

$$\varepsilon^* \downarrow = \frac{F\downarrow(\tau_b) - F\downarrow(\tau_t) + B(\tau_t) - B(\tau_b)}{B(\tau_t) - F\downarrow(\tau_t) + s^*(B(\tau_t) - B(\tau_b))} \tag{26}$$

and

$$\varepsilon^* \uparrow = \frac{F\uparrow(\tau_t) - F\uparrow(\tau_b) + B(\tau_b) - B(\tau_t)}{B(\tau_b) - F\uparrow(\tau_b) + s^*(B(\tau_o) - B(\tau_t))} \tag{27}$$

where

$$s^* = (\bar{\mu}(1 - \omega_0 + 2\omega_0\beta)\tau)^{-1}. \tag{28}$$

The emissivity defined by equations (26)-(28) allow for a non-isothermal structure of the layer. For the case of an isothermal layer, the effective emissivities take the more familiar form of equations (4) and (5).

The effective emissivity of the non-isothermal cloud (equations 26-28) is a function of the cloud temperature structure, optical depth, or LWP and n(r). Equations (26)-(28) indicate that a cloud with a vertically varying LWP will display a variation in the relationship between the LWP and ε^* due to the contribution of equation (28). This is in agreement with the aircraft observations of Curry and Herman (1985), who employ an effective emissivity similar to equations (26) and (27) with $s^* = 0$. In that paper they least square fit the observations of ε^* as an exponential function

of the observed LWP using a flux mass absorption coefficient, K (e.g. equation 17). The largest inter-cloud variation in K occurred for clouds with the largest inhomogeneities in liquid water content. Variations in LWP will result in variations in $(B(\tau_b) - B(\tau_t))/\tau$, and therefore in ε^*. A variation of ε^* with n(r) is contained in the s^* term of equations (27) and (28). This dependency is demonstrated in figure R8 which depicts s^* ($\bar{\mu} = 1.66$, $\tau = 1$) as a function of wavelength for three different size particles: 5, 10 and 30 μm. s^* displays a much greater sensitivity to particle size than either ϱ or KQ_{ext}/Q_{abs}, and is a strong funciton of both the size and wavelength.

For aircraft observations of LW radiative fluxes and cloud microphysical parameters, equations (27)-(28) may improve the parameterization of the effective emissivity versus liquid water path in the form of equation (17). There should also be consistency between a parameterization using equation (17) and the effective emissivity defined by equation (14), which can be determined from the microphysical measurements.

Several parameterization schemes of infrared cirrus radiative properties have been presented in the literature. The most commonly used appear to those using the effective emissivity approach. Parameterization for the emittance, transmitance and reflectance based on theoretical calculations has been given by Liou and Wittman (1979). Wu (1984) took the approach of separating the total cirrus emittance into the absorption emissivity, scattering emissivity and reflection emissivity, and then parameterized each component separately. We'll discuss more about parameterizing after discussing the SW radiative properties. Figures R6-R8 suggest that a simple paramertierization may be difficult.

The IR heating profile within a cirrus cloud is largely determined by the temperature difference between the ground (or underlying cloud) and the cirrus cloud base temperature. Figure R9 shows the in cloud heating rate as a function of the incident flux at cloud base (Ackerman *et al.*, 1988). As the upwelling radiation increases the total heating in the layer increases. In addition, the vertical gradient of the heating increases, increasing the radiative destablization. The effect of cloud thickness on the heating rate is shown in figure R10 for a constant IWC of 0.02 g m^{-3}. The cloud top heating decrease, and eventually becomes cooling as the cloud base is lowered. As the

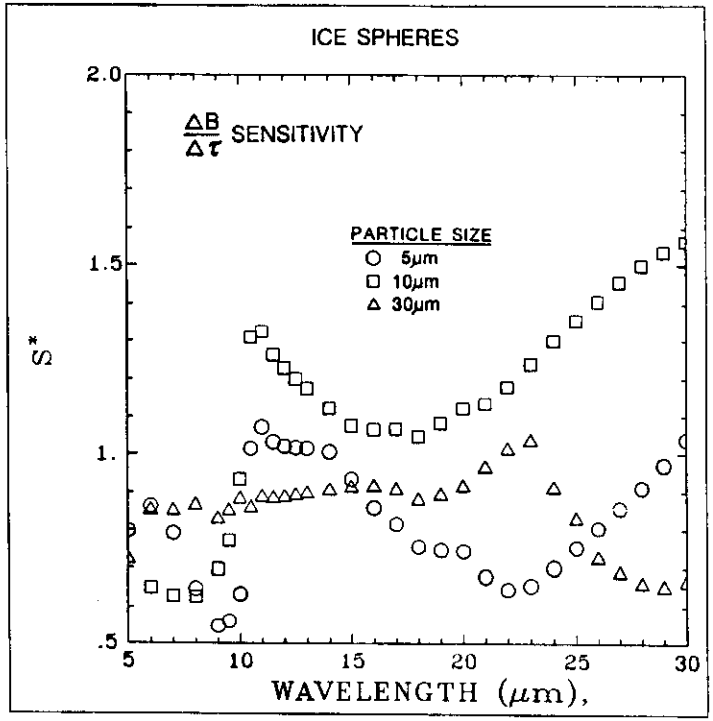

Figure R8

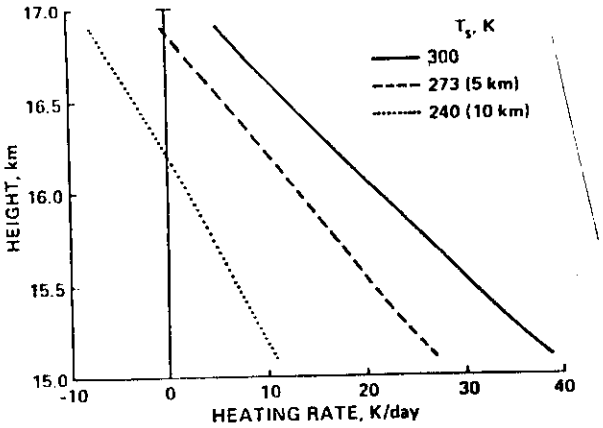

FIG. R9. In-cloud heating rates as a function of height for a cloud subject to upwelling radiation from a clear atmosphere (solid curve), from a 273 K black surface at 5 km (dashed), and from a 240 K black surface at 10 km (dotted). Ackerman et al 1988

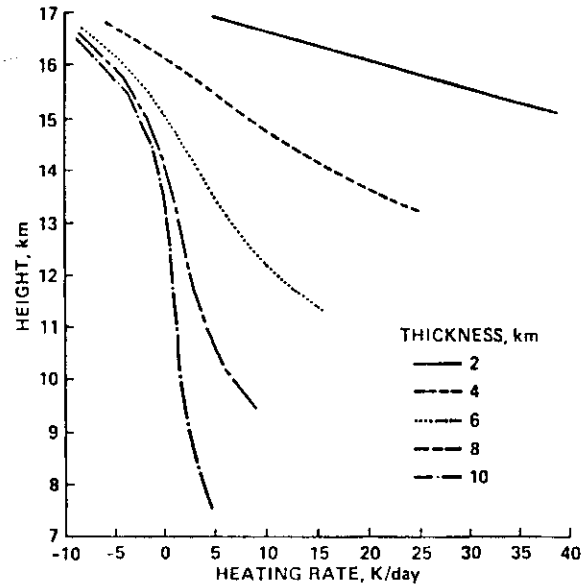

FIG. R10 In-cloud heating rates as a function of height for clouds with a constant IWC and geometric thicknesses ranging from 2 to 10 km. In all cases, cloud top is at 17 km. A. ... J. 1 1988

cloud becomes optically thick, the cloud top cooling asymptotically approaches a value which is dependent on the IWC. The cloud base warming also decrease but at a slower rate. Thus the radiational destabilization is reduced as the cloud is extended. The effect of IWC on the heating rate is demonstrated in figure R11. For thin cirrus there is a uniform heating in the cloud. As the IWC increases the difference between heating near the cloud base and top increases. For a thin cirrus cloud in the subartic winter atmosphere displays a cooling throughout the cloud layer, this would be expected as demonstrated in figure R9. The effect of the vertical distribution of IWC on the heating rates is demonstrated in figure R12. In each case the total optical thickness remains constant.

In addition to affecting the heating rates of the cloud layer itself, the presence of cirrus cloud also modifies the radiative cooling of the stratosphere (Roewe and Liou, 1978) as well as the surface radiative energy budget. Cirrus clouds significantly increase the cooling in the stratosphere above 20 km.

Comparison of the spectral flux divergence figure R13 reveals that heating dominates in the 8-12 μm window region while cooling occurs at the far infrared ($\lambda > 20\mu$m). In the window region radiation incident on the cloud from the troposphere exceeds the radiation which can be emitted by the cirrus cloud. The layer cools at the far infrared because the emission form a cold cloud is greater than the emission from the warmer troposphere at long wavelengths. In the tropical atmosphere the heating in the window dominates the cooling in the far IR, while in the subartic winter case the reverse is true.

The relationship between the window heating and the far IR cooling depends not only on the environmental conditions in which the cloud exists, but also on the microphysics of the cloud. This is demonstrated in Figure R14 (Stackhouse *et al*, 1988). The presence of small particles substantially reduces the the total cloud cooling. This results primarily from an enhanced heating in the window region.

The effect of small particles is also evident in high spectral observations in the 8-12 μm window. Observations by Ackerman *et al* (1989) show spectral variation in equivalent blackbody

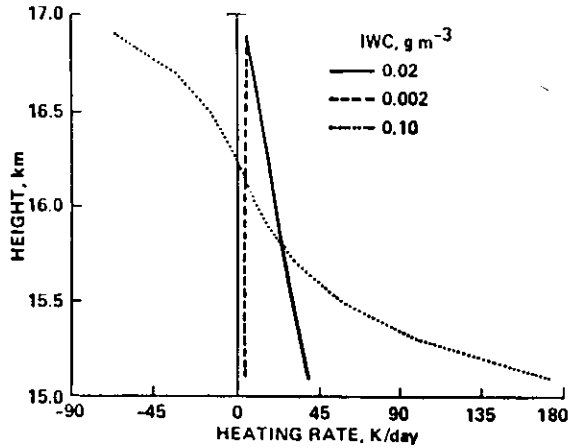

FIG. R11 In-cloud heating rates as a function of height for three constant ice water contents: 0.02 g m^{-3} (solid curve), 0.002 g m^{-3} (dashed), and 0.10 g m^{-3} (dotted). (Note the horizontal scale of this figure is substantially compressed relative to other figures.)

Ackerman et al 1988

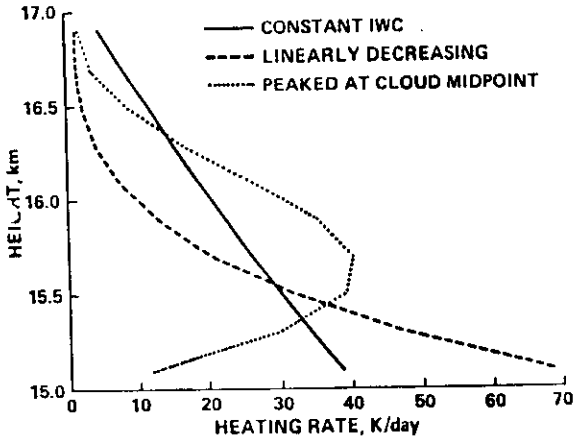

FIG. R12 In-cloud heating rates as a function of height for three IWC profiles all with the same optical depth: constant with altitude (solid curve), linearly decreasing with altitude (dashed), and peaked at cloud midpoint (dotted).

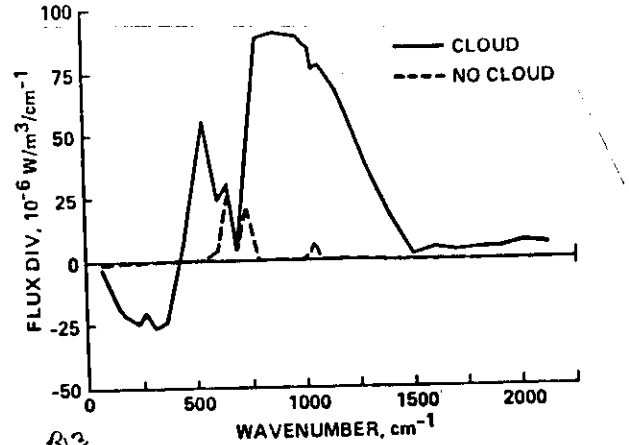

R13

FIG. R14 Flux divergence (in units of -10^6 W m^{-3} cm^{-1}) across the layer between 15 and 17 km as a function of wavenumber. Solid curve is for standard cloud case, dash for no-cloud. Note that positive ordinate values imply heating and negative values imply cooling.

After Ackerman et al 1988

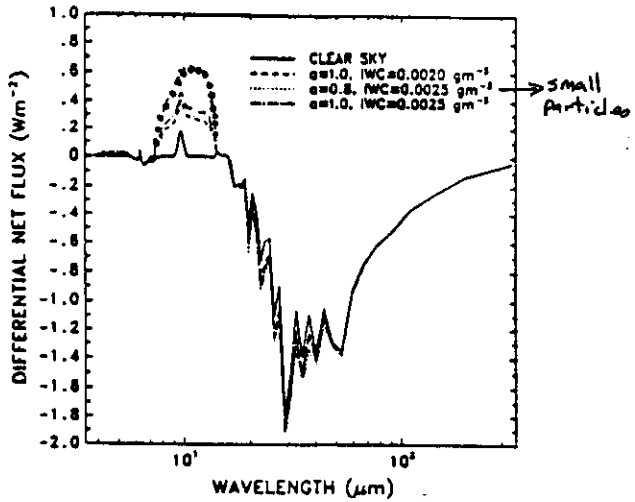

Fig R15 After Stackhouse et al.

temperature in the window region of greater than 5°C for a given cloud (figure R15). Theoretical calculations indicate that the magnitude of the spectra variation in brightness temperature is related to the particle size. The smaller particles are associated with larger brightness temperature differences. The effect of particle shape is also seen in high-resolution IR spectral measurements. Figure R16 depicts the brightness temperature difference between 8 and 11 μm narrow spectral bands, and 11 and 12 μm bands measured with the High-spectral resolution Interferometer Sounder (HIS) (Revercomb *et al*, 1988). The two envelopes are for theoretical calculations assuming spheres and cylinders.

3b. SW Radiative Properties

Observations of cirrus cloud SW properties, such as albedo and absorption are less frequent than the LW observations. Observations of the transmisivity of cirrus clouds at visible wavelengths have been presented by Kondratyev (1969) as a function of solar zenith angle, θ_o. Aircraft observations have been presented by Drummond and Hickey (1971) and Reynolds *et al.* (1975). These study indicated the large variability in the cirrus SW radiative properties. Paltridge and Platt (1981) employed aircraft observations of the solar spectrum and defined the cloud absorptance as

$$a = \frac{[F\downarrow(z_o) - F\uparrow(z_o)] - [F\downarrow(z) - F\uparrow(z)}{F\downarrow(z_o) + F\uparrow(z)} \tag{29}$$

where z_o refers to the top of the cloud. This expression assumes that the same fraction is absorbed for both the upward and downward fluxes. This is not necessarily true due to water vapor absorption. In addition they expressed the cloud albedo as

$$\alpha = \frac{F\downarrow(z_o)(1-a) - F\downarrow(z)}{F\downarrow(z_o) + F\uparrow(z)} \tag{30}$$

which assumes that the diffuse albedo is the same as the direct beam albedo. This expression also has the same approximations and error as in equation (29). The results of these measurement are depicted in figure R17. All points refer to some depth z measured from the top of the cloud. Different symbols represent different day and different solar zenith angles ranging from 36° to

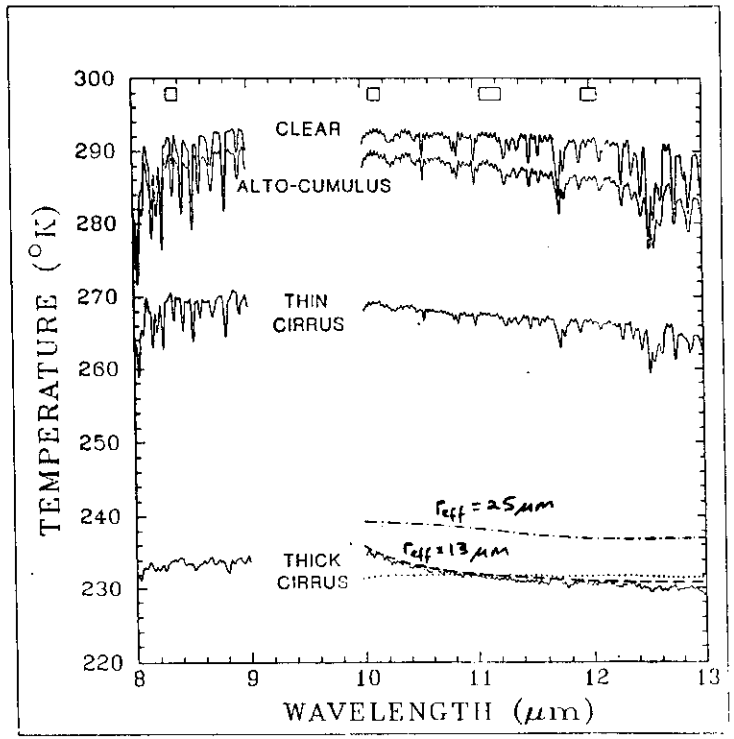

figure R15

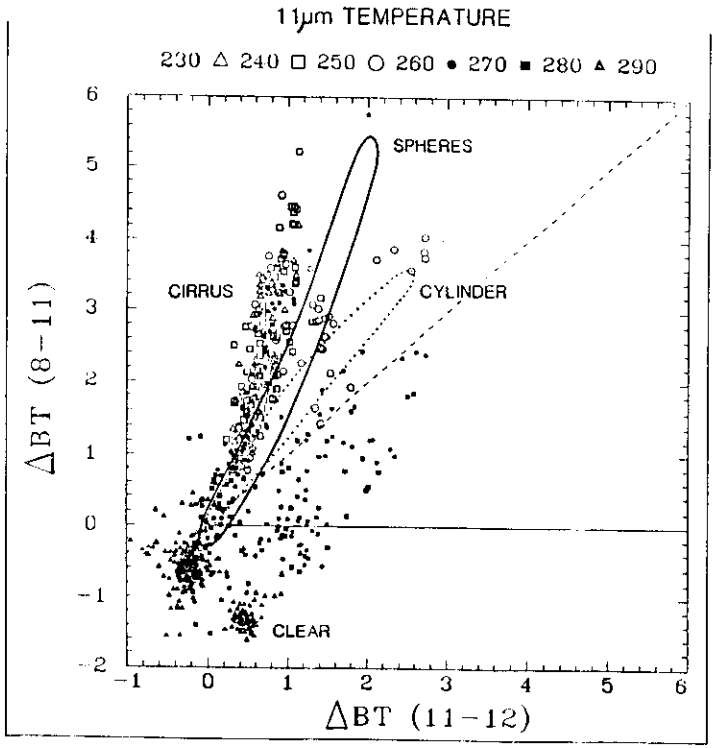

figure R16

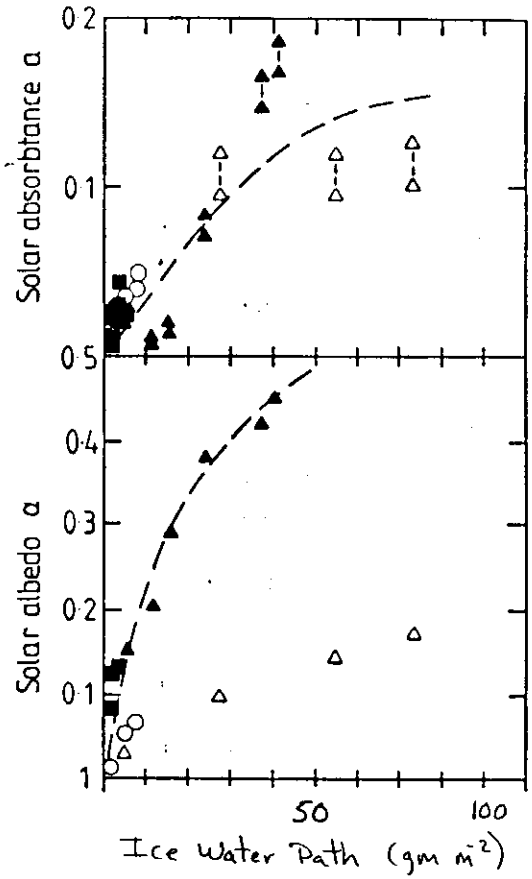

figure R17. Paltridge and Platt 1981

42°. The solar absorptance and albedo are plotted as a function of beam emittance in figure R18. The short wave absorptance increase with emittance. The dashed line represents water vapor absorption of the cloud layer, with the ice particles removed. The difference between the solid line and the dashed is a measure of the extra absorption induced by the cirrus particles. Solar absorption is significant. The solar albedo also increases emittance. The dashed curve is a theoretical calculations assuming cylindrical particles and the dotted curve represents spherical particles for a $\theta_o = 35°$.

Employing aircraft measurements to describe the SW radiative properties of cirrus is complicated by the changing solar geometry. Thus one turns to theoretical calculations. A detailed study of the solar radiative transfer in cirrus clouds consisting of hexagonal ice crystals was presented by Takano and Liou (1989a and b). Due to the computational restrictions results were calculated for a few selected wavelengths.

An example of the effect of IWC on heating rates in cirrus cloud is given in figure R19 (Ackerman *et al.* (1988). Increasing the IWC increases the total heating as well and the vertical difference between cloud top and base. Stackhouse *et al.* (1989) have presented detail calculations of the SW radiative properties of cirrus. The effect of IWC on the solar heating rate for the tropical and subarctic winter conditions were similar to those of Ackerman *et al.* (1988). The effect of particle size on the heating rate is depicted in figure R20. The presence of small particles enhance the cloud heating. The addition of small particles primarily effects those wavelengths greater than 2.8μm. The effect of small particles on spectral albedo is large as demonstrated in figures 21 and 22.

4. Parameterizations

There are two approaches to paramterizing the radiative properties of clouds. In the first, one tries to parameterize the single scattering properties and in the second one attempts to parameterize the bulk radiative properties. As an example of the first, consider the SW properties of water clouds, in which the size parameter is large. A suitable parameterizations is the ADT of van

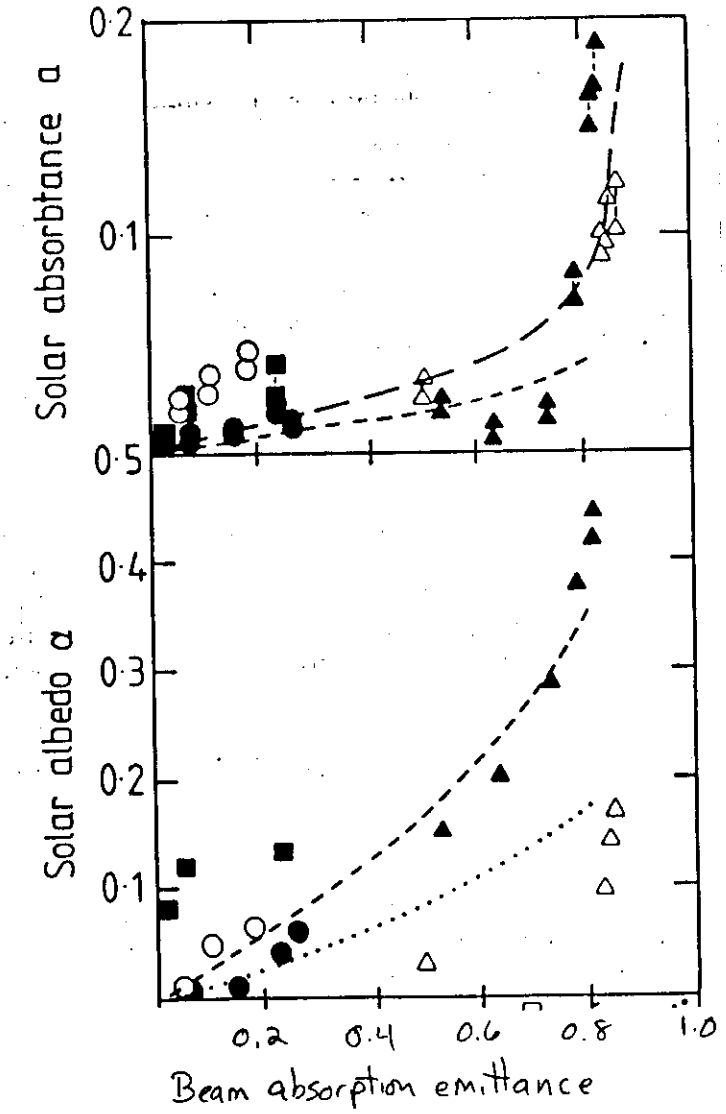

Figure R18 after Paltridge and Platt (1981

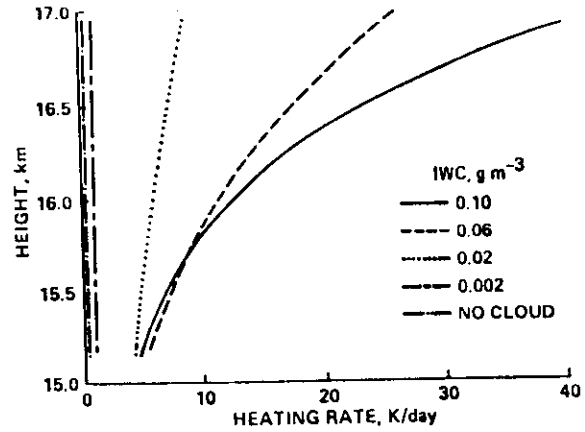

R19 Solar heating rates as a function of height for clear sky and for IWCs of 0.002, 0.02, 0.06 and 0.1 g m^{-3}. The solar zenith angle is 53°. After Ackerman et al

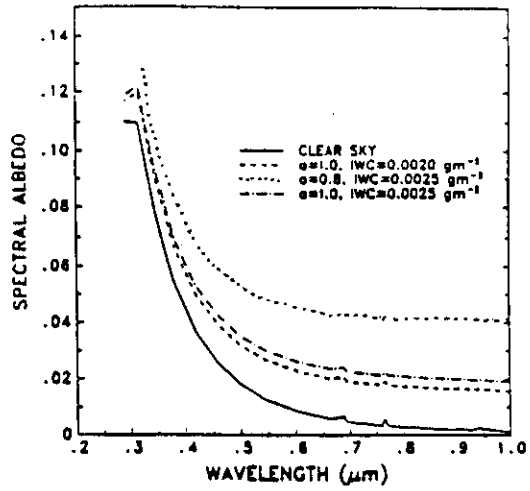

Figure R21. Spectral albedo in the visible wavelengths (0.25 – 1.0μm)for the cases described in text for a 3 km uniform cirrus cloud in a Wisconsin atmosphere.
Stackhouse et al (1989)

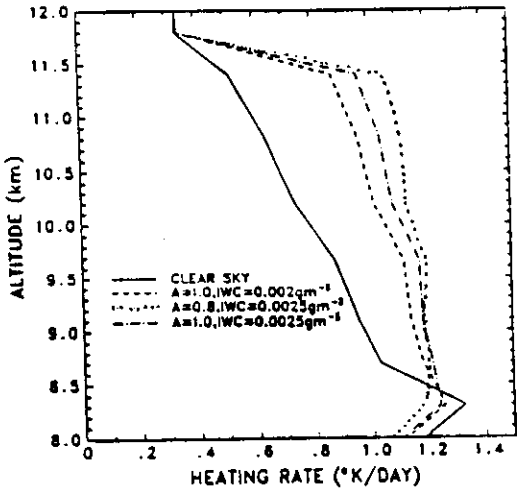

fig. R20 After Stackhouse et al 1989

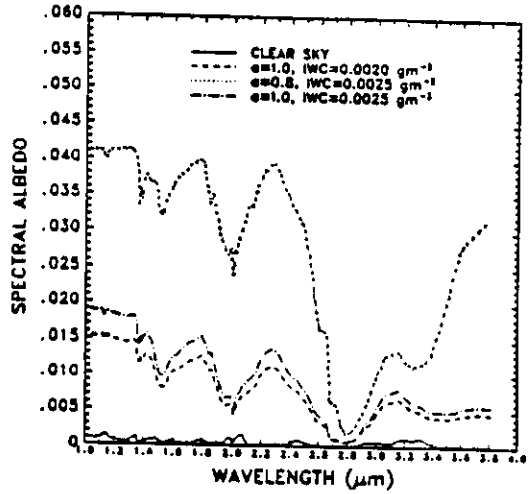

R22
Figure : Spectral albedo in the near infrared (1.0 – 4.0μm) for the cases described in text for a 3 km uniform cirrus cloud in a Wisconsin atmosphere.
Stackhouse et al 1989

de Hulst (1954) or of MADT (Ackerman and Cox, 1988). This type of parameterization is based on the physics of the problem and is therefore independent of radiative transfer models. It also accounts for microphysical changes in the aerosol, such as changes in size distribution or index of refraction and is applicable to dust layers and water clouds. It is likely that the theory can also be applied to large irregular shaped particles, such as ice crystals. An example of the second type is the parameterizations of effective emissivity. While these paramterizations are often simpler they are dependent on the radiative model used, for example the assumption of an isothermal layer.

It is unlikely that climate models will be able to predict ice crystal size and shape. The hope is that a broad parameterization scheme will be appropriate. Whatever the scheme, it is important that there be physical consistency between the LW and SW parameterizations. For example, consider the effect of cirrus clouds on the surface energy budget. It can be shown that if

$$\sigma T_c^4 \Delta\epsilon > (1 - R_g) F_o \Delta R \tag{31}$$

then warming occurs, otherwise cooling results. In equation (31) T_c is the cloud temperature; R_g is the ground reflectance; F_o is the incoming flux; $\Delta\epsilon$ is a change in cirrus cloud emittance and ΔR is the corresponding change in the cloud reflectance. As demonstrated above both ϵ and R are a function of the cloud microphysical properties and are therefore related to each other in some manner. This is also indicated in the measurements of Paltridge and Platt (1981). Parameterizations schemes must treat relationship between $\epsilon - R$ correctly.

6. References

Ackerman, T. P., K. N. Liou F. P. Valero and L. Pfister, 1988: Heating rates in tropical anvils. *J. Atmos. Sci.*, **45**, 1606-1623.

Ackerman, S. A. and G. L. Stephens, 1987: The absorption of solar radiation by cloud droplets: an application of anomalous diffraction theory. *J. Atmos. Sci.*, **44**, 1574-1588.

Asano, S., and G. Yamamoto, 1975: Light scattering by a spheroidal particle. *Appl. Opt.*, **14**, 29-49.

Bohren, G. F. and D. R. Huffman, 1983: *Absorption and Scattering of Light by Small Particles.* J. Wiley and Sons, Inc., 530 pp.

Cai, W. and K. N. Liou, 1982: Polarized light scattering by hexagonal ice crystals: Theory. *Appl. Opt.* **21**, 3569-3580.

Coakley, J.A. and P. Chýlek, 1975: The two-stream approximation in radiative transfer: including the angle of the incident radiation. *J. Atmos. Sci.*, **32**, 409-418.

Coakley, J.A., R.D. Cess and F.B.Yurevich, 1983: The effect of tropospheric aerosols on the earth's radiation budget: A parameterization for climate models. *J. Atmos. Sci.*, **40**, 116-138.

Fouquart, Y. and B. Bonnel, 1980: Computations of solar heating of the earth's atmosphere: A new parameterization. *Beitr. Phys. Atmosph.*, **53**, 35-62.

Hansen, J. E. and L. D. Travis, 1974: Light scattering in planetary atmospheres. *Space Science Reviews*, **16**, 527-610.

King, M.D. and Harshvardhan, 1986: Comparative accuracy of selected multiple scattering approximations. *J. Atmos. Sci.*, **43**, 784-801.

Hemysfield, A. J. and C. M. R. Platt, 1984: A parameterization of the particle size spectrum of ice clouds in terms of the ambient temperature and the ice water content. *J. Atmos. Sci.*, **41**, 846-855.

Heymsfield, A. J. and K. M. Miller, 1989: The October 27-28 1986 FIRE cirrus case study: cloud microstructure. Submitted to *J. Atmos. Sci.*

Liou, K. N., 1972: Light scattering by ice clouds in the visible and infrared: A theoretical study. *J. Atmos. Sci.*, 29, 524-536.

Liou, K. N., 1974: On the radiative properties of cirrus in hte window region and their influence on remote sensing of the atmosphere. *J. Atmos. Sci.*, **31**, 522-532.

Liou, K. N. and G.D. Wittman, 1979: Parameterization of the radiative properties of clouds. *J. Atmos. Sci.*, **36**, 1261-1273.

Liou, K. N., 1986: Review: Influence of cirrus clouds on weather and climate processes: A global perspective. *Mon. Wea. Rev.*., **114**, 1167-1199.

Meador, W.E. and W.R. Weaver, 1980: Two stream approximations to radiatve transfer in planetary atmospheres: A unified description of existing methods and a new improvement. *J. Atmos. Sci.*, **37**, 630-643.

Mie, G., 1906: Contributions to the optics of turbid media, especially colloidal metal solutions. *Ann. Physik.*, **25**, 377-445.

Nussenzveig, H. and W. Wiscombe, 1980: Efficiency factors in Mie scattering. *Phys. Rev. Lett.*, **45**, 1490-1494.

Paltridge, G. W. and C. M. R. Platt, 1981: Aircraft measurements of solar and infrared radiation and the microphysics of cirrus cloud. *Q. J. R. Meteorol Soc.*, **107**, 367-380.

Platt, C. M. R., 1973: Lidar and radiometric observations of cirrus clouds. *J. Atmos. Sci.*, 30, 1191-1204.

Platt, C. M. R. and A. C. Dilley, 1981: Remote sounding of high clouds. IV: Observed temperature variations in cirrus optical properties. *J. Atmos. Sci.*, **38**, 1069-1082.

Platt, C. M. R. and A. C. Dilley, 1984: Determination of cirrus particle single scatter phase function from lidar and radiometric data. *Appl. Optics*, **23**, 380-386.

Platt, C. M. R. and G. L. Stephens,1980: Interpretation of remotely sensed high cloud emittances. *J. Atmos. Sci.* **37**, 2314-2322.

Palmer, K.F. and D. Williams, 1974: Optical Constants of Water in the near Infrared. *J. Opt. Soc. Amer.*, **64**, 1107-1110.

Preisendorfer, R. W., 1960: Application of radiative transfer theory to light measurements in the sea. *International Association of Physical Oceanography*, 11-31.

Revercomb, H. E. , H. Buijs, H. B. Howell, D. D. LaPorte, W. L. Smith and L. A. Sromovsky, 1988: Radiometric calibration of IR Fourier transform spectrometers: solution to a problem with the High-spectral resolution Interferometer Sounder. *Appl. Optics*, **27**, 3210-3218.

Sassen, K. and K. N. Liou, 1979: Scattering of polarized laser light by water droplet mixed phase and ice clouds. Part I: Angular scattering patterns. *J. Atmos. Sci.*, **36**, 838-851.

Schmetz, J. and E. Raschke, 1980: An approximate computation of infrared radiative fluxes in a cloudy atmosphere, *Pageoph*, **119**, 248-258.

Smith, W. L., H. E. Revercomb, H. B. Howell, H. M. Woolf and D. D. LaPorte, 1986: The High resolution Interferometer Sounder (HIS). *CIMSS View*, Vol II, No. 3, University of Wisconsin, Madison, WI.

Spinhirne, J. D. and W. D. Hart, 1989: The October 27-28 1986 FIRE cirrus case study: ER-2 lidar and spectral radiometer cirrus observations. Submitted to *J. Atmos. Sci.*

Starr, D. O. and D. Wiley, 1989: The October 27-28 1986 FIRE cirrus case study: Meteorology and cloud fields. Submitted to *J. Atmos. Sci.*

Stackhouse P. W. and G. L. Stephens, 1989: A theoretical and observationsl comparison of cirrus cloud radiative properties. Colorado State University Report.

Stephens, G. L., 1980: Radiative properties of cirrus clouds in the infrared region. *J. Atmos. Sci.*, **37**, 435-445.

Stephens, G. L., 1978: Radiative properties of extended water clouds. Parts I and II. *J. Atmos. Sci.*, **35**, 2111-2132.

Stephens, G. L., S. A. Ackerman and E. A Smith, 1984: A shortwave parameterization revised to improve cloud absorption. *J. Atmos. Sci.*, **41**, 687-690.

Twomey, S. and C.F. Bohren, 1980: Simple approximations for calculations of absorption in clouds. *J. Atmos. Sci.*, **37**, 2086-2094.

van de Hulst,H. C., 1957: ***Light Scattering by Small Particles.*** (Second ed. 1981) Dover, New York, 447 pp.

Volkovitskiy, O. A., L. N. Pavlova, and A. g. Petrushin, 1980: Scattering of light by ice crystals. *Atmos. Ocean. Phys*, **16**, 90- 102.

Wait, J. R., 1955: Scattering of a plane wave from a circular dielectric cylinder at oblique incidence. *Can. J. Phys.*, **33**, 189-195.

Wiscombe, W., and G. W. Grams, 1976: The backscattered fraction in two-stream approximations. *J. Atmos. Sci.*, **33**, 2440-2451.

Wu, M. L. C., 1984: Radiative properties and emissivity parameterization of high level thin clouds. *J. Climate Appl. Meteor.*, **23**, 1138-1147.